

# Thermooxidative Aging of Polyoxymethylene, Part 2: Embrittlement Mechanisms

B. Fayolle,<sup>1</sup> J. Verdu,<sup>1</sup> D. Piccoz,<sup>2</sup> A. Dahoun,<sup>3</sup> J. M. Hiver,<sup>3</sup> C. G'ssell<sup>3</sup>

<sup>1</sup>Laboratoire Ingenierie des Matériaux, UMR 8006 CNRS–Arts et Métiers Paristech 151 Bd de l'Hôpital, 75013 Paris, France

<sup>2</sup>AREVA, T&D Boulevard de la résistance, BP 84019, 71040 Mâcon, Cedex 9, France

<sup>3</sup>Laboratoire de Physique des Matériaux, UMR 7556 CNRS–Nancy Université INPL, Ecole des Mines de Nancy, Parc de Saurupt, 54042 Nancy Cedex, France

Received 19 December 2007; accepted 2 June 2008

DOI 10.1002/app.29126

Published online 9 October 2008 in Wiley InterScience (www.interscience.wiley.com).

**ABSTRACT:** The thermal oxidation at 130°C of polyoxymethylene homopolymer (H) and copolymer (C) samples of close initial molar masses has been studied by gravimetry, rheometry, X ray scattering, and tensile testing. Both samples undergo random chain scission and depolymerization. Their crystallinity ratio increases, whereas their long period decreases. All these changes are faster for H than for C. Tensile tests reveal that there is no significant change of behavior law except for the ultimate strain, which decreases abruptly when the weight average molar mass reaches a value of the order of 70 kg mol<sup>-1</sup> for H

and 90 kg mol<sup>-1</sup> for C. At these molar masses values, the entanglement network of the amorphous phase has undergone only small damage. In contrast, a chemi-crystallization process has induced significant morphological changes, especially a decrease of the interlamellar thickness. It is suggested that this latter phenomenon could be responsible for embrittlement. © 2008 Wiley Periodicals, Inc. *J Appl Polym Sci* 111: 469–475, 2009

**Key words:** polyoxymethylene; thermal oxidation; morphology; embrittlement

## INTRODUCTION

The first part of this article was devoted to the study of chemical aspects of polyoxymethylene (POM) thermal oxidation in solid state.<sup>1</sup> It was found that POM degrades through a radical chain mechanism with the following main characteristics:

- i. Hydroperoxides (POOH) are very unstable, and their decomposition induces systematically a random chain scission.
- ii. But POOH decomposition induces also a depolymerization responsible for weight loss.

A kinetic model was established from the experimental observations and predicts well the structural changes for unstabilized POM homopolymer.

This (second) part of the article is aimed to answer the following question: Can the kinetic model predict the polymer embrittlement? Because the principle of the model is to avoid empirism, the answer must be non empirical. However, embrittlement mechanisms are not well established for polymers

such as POM. In the case of amorphous polymers or semicrystalline polymers having their amorphous phase in glassy state, for instance PET,<sup>2</sup> embrittlement is observed when the molar mass  $M'_C$  reaches a value of the order of the entanglement molar mass  $M_e$ , for instance  $M'_C \sim 5M_e$ .<sup>3</sup> This means that a non-negligible part of entanglement network is seriously damaged and cannot efficiently transmit stresses to the crystalline phase.

Semicrystalline polymers having their amorphous phase in rubbery state have clearly a distinct behavior: In these cases, the embrittlement molar mass ( $M'_C$ ) is considerably higher than the entanglement molar mass ( $M_e$ ):  $M'_C \sim 20$  to  $50 M_e$ .<sup>4,5</sup> This means that embrittlement occurs while the entanglement network has suffered only very little damage. Tie chains play an important role in plastic polymer behavior but there is no reason to suppose that they have reactivity toward oxidation higher than the other amorphous chains, so that the proportion of broken tie chains is expected to be very low. There is no way apparently to explain embrittlement of these polymers by a direct effect of molar mass change.

It is well known, however, that in these polymers, chain scission induces chemi-crystallization<sup>6–10</sup> i.e., morphological changes which can affect the fracture behavior. In the case of polyethylene<sup>11</sup>, it has been

Correspondence to: B. Fayolle (bruno.fayolle@paris.ensam.fr).

recently proposed that the causal chain of embrittlement during oxidation aging in solid state could be:

Oxidation → Chain scission → chemi-crystallization → reduction of the interlamellar distance → embrittlement.

The aim of this article is to try to express quantitatively the above relationships between structural changes induced by thermal-oxidation and mechanical properties evaluated by tensile testing. For this purpose, aging experiments at 130°C on one POM homopolymer and one POM copolymer were performed.

## EXPERIMENTAL

The experiments were conducted with samples of 1-mm thick obtained by injection molding of a homopolyoxymethylene (Delrin100) supplied by Dupont and a copolyoxymethylene (Hostaform) supplied by Ticona. Average molecular weights of the polymers were, respectively:  $M_n \sim 70 \text{ kg mol}^{-1}$  and  $M_w \sim 140 \text{ kg mol}^{-1}$  for Delrin,  $M_n \sim 60 \text{ kg mol}^{-1}$  and  $M_w \sim 120 \text{ kg mol}^{-1}$  for Hostaform.

Isothermal aging tests were performed under ambient air (0.02 MPa) at 130°C. Homogeneity of degradation in the sample thickness was checked by using mapping IR measurements with the help of an optical microscope coupled with a motorized X-Y scale, with distance increments of 10  $\mu\text{m}$ . A Bruker IFS 28 spectrophotometer with a resolution of 4  $\text{cm}^{-1}$  was used for infrared measurements. Homogeneity of degradation in the sample thickness is checked by using mapping IR measurements with the help of an optical microscope coupled with a motorized X-Y scale, with distance increments of 10  $\mu\text{m}$ . No formate profile has been put in evidence for all samples.<sup>1</sup> As a result, degradation can be considered as homogeneously distributed in the sample thickness for the aging condition and the sample thickness under study.

Wide-angle X-ray scattering (WAXS) and small-angle X-ray scattering (SAXS) were used to study the crystalline structure of the polyoxymethylene grades by means of a 2D diffraction system (Inel, France) equipped with a copper anode. The selected tension and the intensity are 30 kV and 40 mA, respectively. The wavelength used is  $K_{\alpha 1}$  copper radiation ( $\lambda_{\text{Cu}\alpha 1} = 0.154 \text{ nm}$ ), selected by means of a parabolic multilayer mirror (Osmic) and a very thin capillary. The 2D transmission pattern is revealed with a scanner that digitalized it with a resolution of 25 microns. The diffraction intensity is corrected by the Lambert equation  $I = I_0 \exp(-\mu t / \cos(2\theta))$  where  $2\theta$  is the diffraction angle,  $\mu$  the absorption coefficient equal in this case to 11.204  $\text{cm}^{-1}$ <sup>12</sup> and  $t$  the thickness of the samples. The latter are parallelepipedic with a thickness of 0.8 mm. Subsequently for

the WAXS analysis, the corrected diffraction curve,  $I(2\theta)$ , is analyzed using PeakFit software (SPSS Inc) in view of extracting the different components: (i) background, (ii) crystalline peaks and (iii) amorphous halo. We calculate crystallinity ratio ( $x_c$ ) from the relative area of crystalline peaks divided this area plus amorphous halo area. SAXS is analyzed using PeakFit software and modified by the Lorentz correction. Subsequently, the long period ( $l_p$ ) is calculated by using the following relationship  $l_p = 2. \lambda_{\text{Cu}\alpha 1} . L / (\Delta\theta)$  where  $L$  is chamber length (804 mm) and  $\Delta\theta$  is the distance between peaks obtained from corrected diffraction curve  $I(2\theta)$  after derivation. The thickness  $l_a$  of the amorphous layer separating adjacent lamellae was estimated using  $l_a = (1 - x_c) l_p$  with  $x_c$  being expressed in terms of mass fraction.

Rheological measurements were performed in dynamic oscillatory mode with a Rheometric Scientific ARES rheometer using parallel plates geometry (plate diameter 25 mm and gap 0.5 mm), at atmospheric pressure. The frequency range is between 0.1 and 100  $\text{rad s}^{-1}$  and the maximum strain amplitude is optimized to measure reliable torque values in the Newtonian domain. Viscosity measurements were performed at 190°C under nitrogen to avoid oxidation during measurements. The molar mass distribution was determined from the viscoelastic spectrum, using the Mead's model.<sup>1,13</sup>

The mechanical tests were carried out on a tensile testing machine INSTRON 4502, at 80°C, with a constant crosshead displacement rate of 10  $\text{mm min}^{-1}$ . Dumbbell shaped specimens having a calibrated length of 25 mm and a width of 4 mm, were cut from the injection molded samples in the flow direction with a MTS H2 stamp. Only engineering strains are reported, no corrections will be made for thickness or width changes induced by necking.

## RESULTS

### Weight changes

The kinetic curves of weight changes are shown in Figure 1. Both kinetic curves display a pseudo induction period during which weight loss is auto-accelerated, followed by a steady state period during which weight loss rate is almost constant. These weight losses are essentially linked to formaldehyde (F) assuming that depolymerization is the main volatile source.<sup>14</sup> Induction times corresponding to the beginning of the steady state are of the order of 800 h for H and 2500 h for C. Weight loss rates in steady state are of the order of 240  $10^{-4}$  percent  $\text{h}^{-1}$  for H, that corresponds to 2.2  $10^{-6}$   $\text{mol kg}^{-1} \text{ s}^{-1}$  of formaldehyde evolution rate ( $dF/dt$ ). For C, the steady state weight loss rate is about 6  $10^{-4}$  percent  $\text{h}^{-1}$ , that

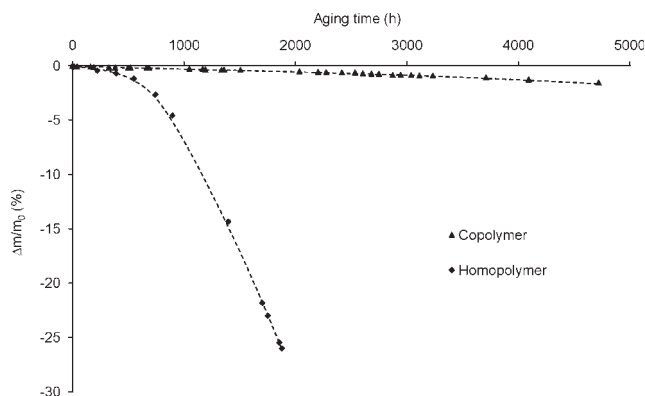


**Figure 1** Kinetic curves of mass loss at 130°C in air at atmospheric pressure.

corresponds to  $5.5 \cdot 10^{-8} \text{ mol kg}^{-1} \text{ s}^{-1}$  of formaldehyde evolution rate.

### Molar mass changes

Molar mass changes during exposure for both POM are illustrated in Figure 2. It appears clearly that  $M_W$  and  $M_n$  decrease during thermal oxidation for both polymers that confirms the predominance of a chain scission process on a crosslinking process. Indeed, the latter process should lead to a molar mass increase which is not consistent with the experimental data. Because crosslinking can be considered as negligible,<sup>1</sup> the number of chain scissions per mass unit ( $s$ ) is given by:

$$s = 2 \left( \frac{1}{M_W} - \frac{1}{M_{W0}} \right) \quad (1)$$

Where  $M_W$  is the weight average molar mass during exposure and  $M_{W0}$  is the initial weight average molar mass.

$s$  has been plotted against exposure time in Figure 3. The homopolymer degrades faster than the copoly-

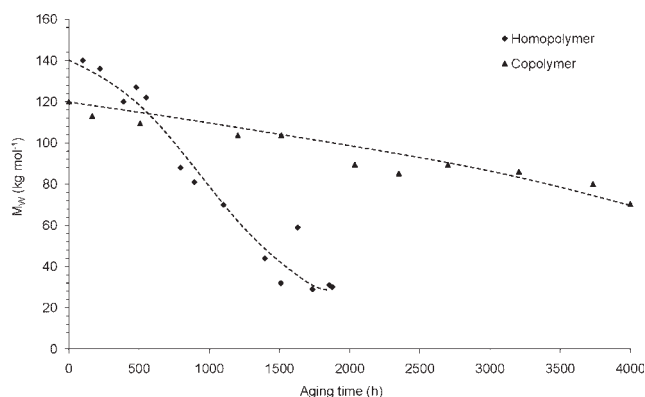


**Figure 2** Weight average molar mass ( $M_W$ ) as a function of aging time.

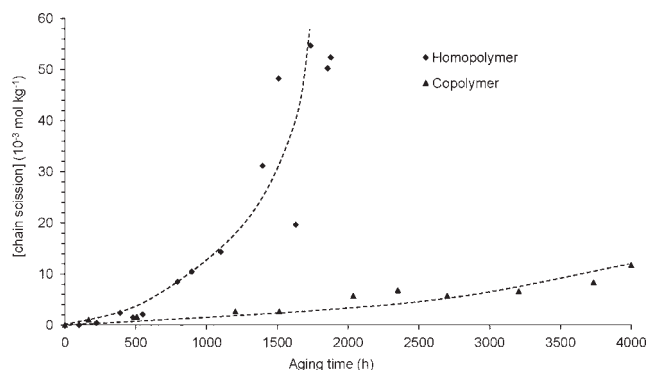


**Figure 3** Number of chain scission against exposure time at 130°C.

mer, the steady state rates of chain scission ( $ds/dt$ ) are of the order of  $167 \cdot 10^{-10} \text{ mol kg}^{-1} \text{ s}^{-1}$  for H and  $5.55 \cdot 10^{-10} \text{ mol kg}^{-1} \text{ s}^{-1}$  for C.

One can define by the ratio  $\lambda$  between rate of formaldehyde and rate of chain scission as follows:

$$\lambda = \frac{dF}{dt} \bigg/ \frac{ds}{dt} \quad (2)$$

During the steady state,  $\lambda$  is close to 132 for H and 100 for C. These values are close to the previously found one.<sup>1</sup> Because there is probably one random chain scission per initiation event (hydroperoxides decomposition),  $\lambda$  can be considered as the kinetic chain length of depolymerization. Surprisingly, it is about the same in homo and copolymer, whereas, in this latter, the comonomer is expected to interrupt the propagation of depolymerization and thus to lower  $\lambda$ . Here, no doubt, H and C differ essentially by the initiation rate, probably due to the stabilizer efficiency in sample C. Indeed, the above results do not permit to conclude about an eventual difference of intrinsic stability between homo and copolymers.

### Morphology changes

X ray scattering has been used to determine the crystallinity ratio  $x_C$  using WAXS and the long period  $l_p$  using SAXS. The thickness  $l_a$  of the amorphous layer separating adjacent lamellae was estimated using  $l_a = (1 - x_C)l_p$  with  $x_C$  being expressed in terms of mass fraction.

$x_C$  was plotted against exposure time in Figure 4. In the case of Homopolymer,  $x_C$  increases at almost constant rate between 0 and 1000 h from 0.57 to 0.69. In the case of copolymer,  $x_C$  increases rapidly during the first 500 h and then reaches a plateau value close to 0.61 and increase after 0.65. Figure 5 illustrates morphology changes for the lamellar structure. The long period  $l_p$  can be considered as

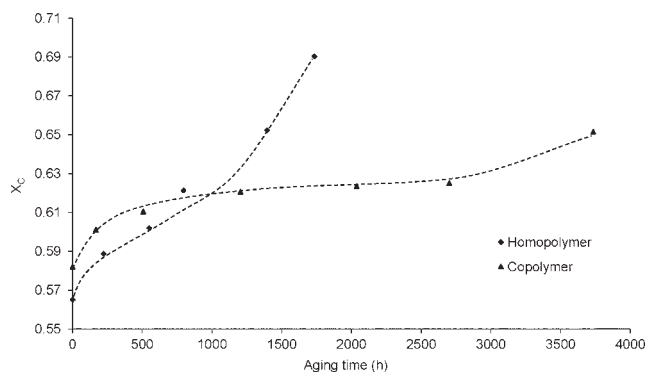


**Figure 4** Crystallinity ratio determined by WAXS as a function of aging time.

constant during aging [Fig. 5(a)]. However, after the initial period dominated by annealing effects,  $l_a$  tends to decrease for both polymers [Fig. 5(b)]. If annealing process would occur during the first stage of aging (typically between 0 and 100 h), a crystallization process inducing  $l_a$  decrease linked to oxidation is put in evidence, especially for homopolymer.

### Embrittlement

Initial tensile curves are presented in Figure 6 for H and 7 for C. Both polymers display a ductile behavior at the test temperature (80°C). H is brittle at ambient temperature in the same tensile testing conditions, whereas C keeps some ductility. Necking process is more diffuse in H than in C, as evidenced by the absence in H and the presence in C of a “knee” in the engineering stress-strain curve.

The failure envelope corresponding to ultimate stress ( $\sigma_R$ ) versus ultimate strain ( $\epsilon_R$ ) for every individual test is presented in Figure 6 for H and in Figure 7 for C. Whereas the curves illustrate the tensile behavior before aging, each point corresponds to the rupture of each tested sample after aging. Time of exposure for some points is also included in these figures.

As previously found for many polymers in the case of a chain scission,<sup>4,15</sup> this failure envelope exhibits the same shape than the virgin polymer tensile curve. As a consequence,  $\sigma_R$  is almost constant as long as plastic deformation subsists so that only ultimate strain  $\epsilon_R$  is a pertinent quantity to characterize aging effects. The ductile-brittle transition can be defined as the state where plastic deformation vanishes i.e., where  $\epsilon_R$  becomes equal to the initial yield strain  $\epsilon_Y$ . This latter is close to 9% for H and 15% for C.

The ultimate strain has been plotted against exposure time, using logarithmic scale for  $\epsilon_R$ , in Figure 8. This figure puts in evidence two very important characteristics of polymer aging with predominant chain scission:

- Transition from a ductile to a brittle behavior is sharp.
- In brittle regime,  $\epsilon_R$  decreases very slowly with exposure time i.e., with conversion of the degradation process.

At last, according to the previous results, it is not surprising to find that embrittlement is sooner in H ( $\sim 1000$  h) than in C ( $\sim 2500$  h).

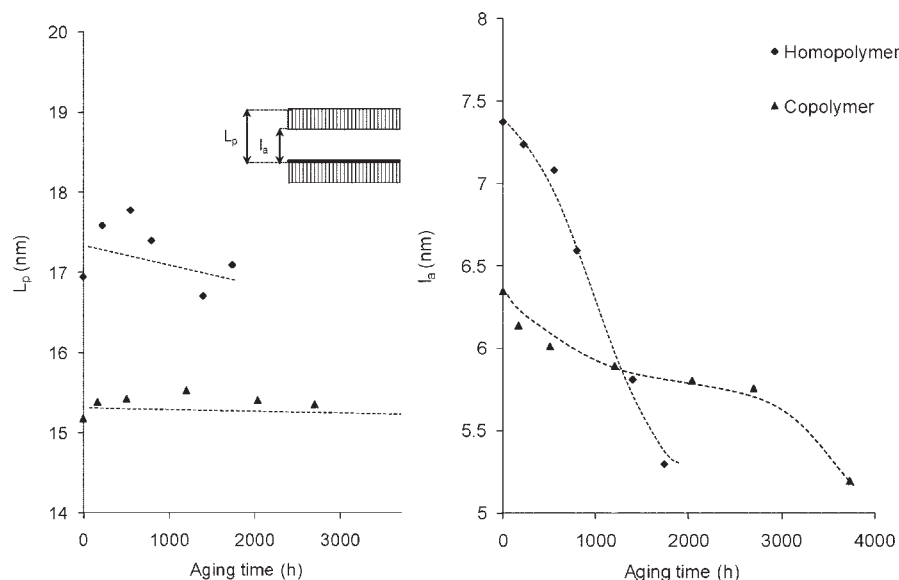


**Figure 5** (a) Long period ( $l_p$ ) for homopolymer and copolymer (respectively,  $\blacklozenge$  and  $\blacktriangle$ ), (b) amorphous layer ( $l_a$ ) for homopolymer and copolymer (respectively,  $\blacklozenge$  and  $\blacktriangle$ ) as a function of aging time.

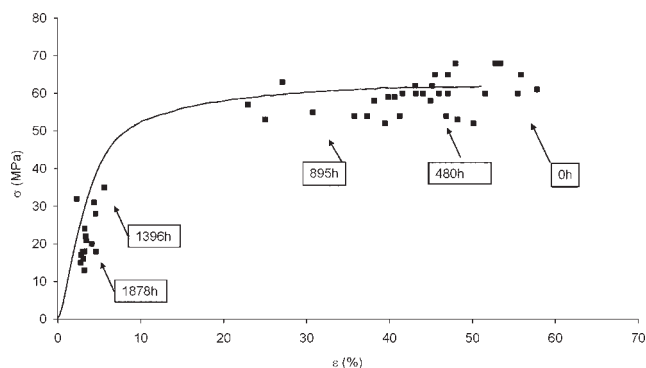


**Figure 6** Tensile behavior of unaged POM Homopolymer (curve) at 80°C and the failure envelope (points): ultimate stress ( $\sigma_R$ ) against ultimate strain ( $\epsilon_R$ ) for different exposure times.

**DISCUSSION**

In the case where POM samples are exposed in air, at temperatures lower than the POM melting point (170°C for H, 163°C for C), degradation results essentially from radical oxidation and leads to random chain scission.<sup>1</sup> This latter liberates progressively chain segments “trapped” by entanglements and allows them to integrate the crystalline phase. This chemi-crystallization process has been described in numerous cases of degradation.<sup>6–10</sup>

Chemi-crystallization characteristics can be tentatively derived from available structure-molar mass relationships<sup>16</sup> assuming that, at a given temperature (here 130°C), an “equilibrium morphology,” which is a material characteristic, is reached when the exposure time becomes longer than the polymer terminal relaxation time. Rault<sup>16</sup> has shown that these relationships are valid as well for “cold” as for “hot” crystallization. So that, there is no reason to suppose that a degraded sample would behave differently as a virgin sample of same molar mass.

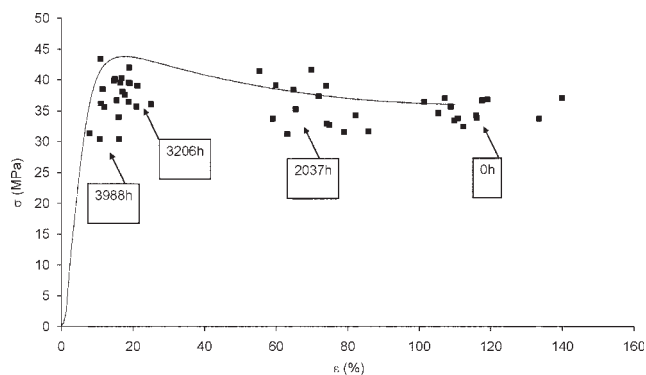


**Figure 7** Tensile behavior of unaged POM Copolymer (curve) at 80°C and the failure envelope (points): ultimate stress ( $\sigma_R$ ) against ultimate strain ( $\epsilon_R$ ) for different exposure times.

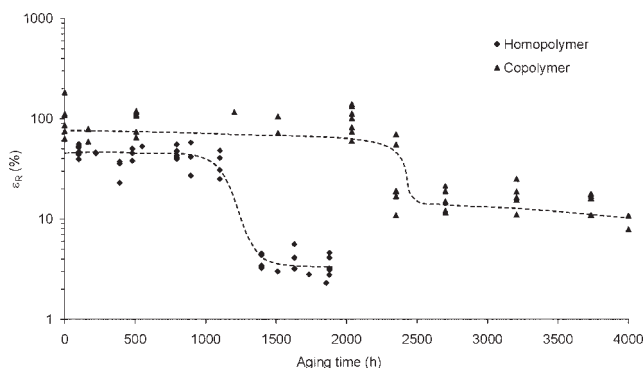


**Figure 8** Changes of ultimate strain  $\epsilon_R$  during exposure at 130°C.

At a given temperature and after the end of the annealing process, the thickness of lamellae  $l_C$  would be independent of molar mass whereas the thickness  $l_a$  of amorphous layers would be given by:

$$l_a = l_{a0} + \alpha \sqrt{M_W} \tag{3}$$

Where  $l_{a0}$  and  $\alpha$  are material dependant parameters after annealing process.

To check the previous relationship,  $l_a$  has been plotted as a function of  $M_W^{1/2}$  in Figure 9. Indeed, we observe experimental data are well described by the relationship (3). Because  $M_W$  can be linked to the number  $s$  of chain scissions, it becomes possible now to establish a link between the chemical degradation and the morphological change. From (1),  $M_W$  can be expressed as a function of chain scission ( $s$ ):

$$M_W = \frac{M_{W0}}{1 + \frac{sM_{W0}}{2}} \tag{4}$$

With  $M_{W0}$  is the weight average molar mass before chain scission process.

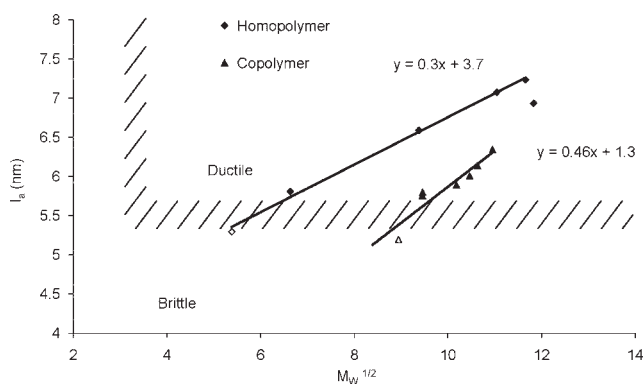


**Figure 9** Shape of the ductile (D)—brittle (B) transition in the plane ( $l_a - M_W$ ). For homopolymer: (◆) ductile behavior (◇) brittle behavior and for copolymer: (▲) ductile behavior (△) brittle behavior.

As a result, one obtains  $l_a$  as a function of  $s$  by using (3) and (4):

$$l_a = l_{a0} + \alpha \left( \frac{M_{w0}}{1 + \frac{sM_{w0}}{2}} \right)^{1/2} \quad (5)$$

Another way to characterize the chemi-crystallization process consists to assess the number  $m$  of the monomer units entering the crystalline phase per chain scission. Let us consider the case of H for instance. According to Figure 4, the rate of crystallinity ratio change in the steady state is:

$$\frac{dx_C}{dt} = 2 \cdot 10^{-8} \text{ s}^{-1}$$

Where  $x_C$  is expressed in terms of mass fraction.

This means that the number of monomer POM units ( $m$ ) entering the crystalline phase is:

$$\frac{dm}{dt} = \frac{1}{30 \cdot 10^{-3}} \frac{dx_C}{dt} = 6.9 \cdot 10^{-1} \text{ mol kg}^{-1} \text{ s}^{-1}$$

The number of monomer units entering the crystalline phase per chain scission in steady state is thus:

$$\mu = \frac{dm}{dt} / \frac{ds}{dt} \sim 40 \text{ monomer POM units per chain scission}$$

In the case of sample C, the determination is more difficult owing to the low rate of crystallinity increase in steady state. A rough determination gives:

$$\frac{dm}{dt} \sim 8 \cdot 10^{-10} \text{ s}^{-1}$$

so that

$$\frac{dx_C}{dt} \sim 2.8 \cdot 10^{-8} \text{ mol kg}^{-1} \text{ s}^{-1}$$

And thus  $\mu \sim 51$ , i.e., a value of the same order as for H.

This chemi-crystallization process induces, as expected, a change in lamellar dimensions, especially a decrease of the amorphous layer thickness. At this state of our investigation, we have a reasonable interpretation of the changes in molar mass and in crystalline morphology, the latter resulting from former ones. But which change is responsible for embrittlement?

The first possible way of explanation is a direct effect of molar mass changes on fracture properties: chain scission destroys the entanglement network in the amorphous phase (entanglement network has

been rejected into the amorphous region of POM during crystallization process<sup>17</sup>). Beyond a certain degree of degradation, disentanglement by chain pull out becomes very easy, the amorphous network becomes too unstable to transmit stresses to the crystalline phase and cavitation initiates easily in the interlamellar regions, promoting thus brittle fracture.

To check this hypothesis, we have plotted the ultimate elongation against weight average molar mass in Figure 10. These results call for the following remarks:

- i. There is clearly a critical molar mass  $M'_C$  separating the brittle and ductile regimes for both POM.
- ii. There is significant difference between  $M'_C$  values for H ( $\sim 70 \text{ kg mol}^{-1}$ ) and for C ( $\sim 90 \text{ kg mol}^{-1}$ ).
- iii. The  $M'_C$  value is considerably higher than the entanglement molar mass ( $M_e = 3 \text{ kg mol}^{-118}$ )

However, the fact that there is no a single  $M'_C$  value seems to indicate that molar mass decrease is not the unique cause of embrittlement. The fact that  $M'_C \gg M_e$  indicates that embrittlement occurs while the entanglement network has undergone only a very small damage: less than 10% of the entanglement strands broken at the ductile-brittle transition. It is noteworthy that this result i.e.,  $M'_C \gg M_e$  seems to be a general property of semicrystalline polymers having a rubbery amorphous phase, for instance polyethylene,<sup>11</sup> polypropylene,<sup>5</sup> or polytetrafluoroethylene.<sup>4</sup> Most of the other polymers especially amorphous ones, seem to have a value close to  $M_e$  ( $M'_C \sim 5M_e^3$ ).

It appears thus that the degradation of the entanglement network in the amorphous phase can not be the direct cause of embrittlement. The change in lamellae dimensions and its consequences on deformation micromechanisms at the lamellae scale could be a possible cause of embrittlement. From a careful

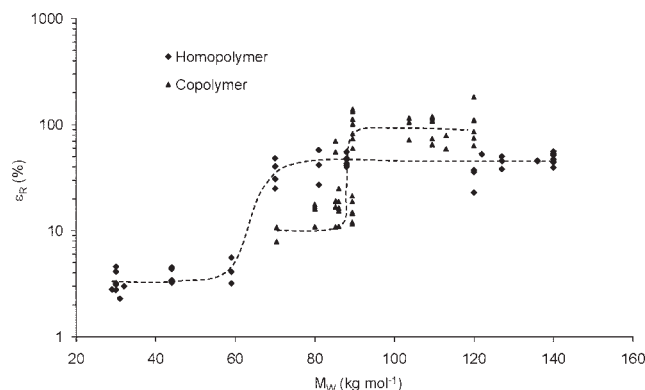


**Figure 10** Strain at break as a function of weight average molar mass.

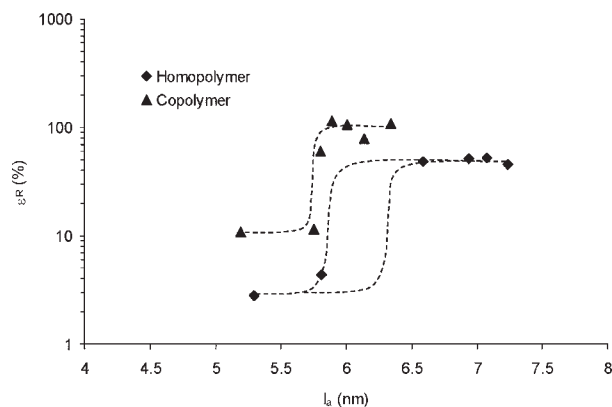


**Figure 11** Strain at break as a function of amorphous layer ( $l_a$ ).

study of PE samples with molar masses in the 50–100 kg mol<sup>-1</sup> range, Kennedy et al.<sup>19</sup> have shown that ductile-brittle transition can occur for various values of the molar mass but it occurs systematically for an amorphous layer thickness  $l_a$  close to 6–7 nm. There is no way to observe ductility for  $l_a$  values lower than 6 nm, and there is no way to obtain  $l_a$  values higher than 6 nm for molar mass lower than 50 kg mol<sup>-1</sup> because PE crystallization is too easy for low molar mass samples.

It seemed to us interesting to plot ultimate elongation  $\epsilon_R$  as a function of  $l_a$  for some degraded samples (Fig. 11). Although more experimental points would be needed to precisely determine the ductile-brittle transition, especially for H, one can see that the critical amorphous layer thickness is between 5.5 and 6.5 nm for both polymers, that seems to be consistent with the hypothesis that embrittlement results from chemi-crystallization and occurs when the amorphous layer thickness becomes lower than 6 ± 0.5 nm whatever the initial POM structure.

The polymer history during aging can be described by a ( $l_a$  versus  $M_W^{1/2}$ ) map (Fig. 9). In this map the ductile-brittle transition would be a horizontal straight line in the whole molar mass domain above the entanglement threshold  $M'_{CO} \sim 5M_e$  (15 kg mol<sup>-1</sup> for POM). Below this limit, the ductile—brittle transition would be represented by a vertical straight line at  $M_W = M'_{CO}$ , but this boundary is virtual because POM crystallization is too fast to allow to achieve samples of low molar mass, for instance 20 kg mol<sup>-1</sup>, with  $l_a$  values higher than 6 nm. The aging trajectories of samples H and C are clearly different and cross the ductile-brittle boundary at different molar mass values,  $M'_C$  being lower for H than for C.

## CONCLUSIONS

The thermal oxidation of polyoxymethylene homo and copolymer samples in air at 130°C, has been

studied by gravimetry, rheometry, WAXS and SAXS, and tensile testing. Both samples undergo random chain scission, depolymerization, and chemi-crystallization processes. The copolymer degrades at a noticeable lower rate than homopolymer, presumably because it contains an efficient stabilizing system, but the yield of depolymerization and chemi-crystallization, expressed in terms of number of events per random chain scission are similar, showing that there is no fundamental difference in degradation mechanisms. Furthermore, a direct relationship between amorphous layer thickness and molar mass has been put in evidence for both POM under study. At last, Embrittlement occurs suddenly at a critical molar mass which differs with initial structure: about 70 kg mol<sup>-1</sup> for homopolymer and 90 kg mol<sup>-1</sup> for copolymer. In contrast, the critical thickness of the amorphous layer  $l_a$  is almost the same: 6 ± 0.5 nm for both polymers. It is concluded that the causal chain leading to POM embrittlement is: oxidation → random chain scission → chemi-crystallization → decrease of the interlamellar thickness → embrittlement. This mechanism leads to consider the ductile-brittle boundary in a two dimensions map ( $l_a - M_W$ ). Future works will be deals with damage-mechanisms occurring during tensile deformation.

## References

- Fayolle, B.; Verdu, J.; Bastard, M.; Piccoz, D. *J Appl Polym Sci* 2008, 107, 1783.
- Wang, W.; Taniguchi, A.; Fukuhara, M.; Okada, T. *J Appl Polym Sci* 1998, 67, 705.
- Sha, Y.; Hui, C. Y.; Ruina, A.; Kramer E. J. *Macromolecules* 1995, 28, 2450.
- Fayolle, B.; Audouin, L.; Verdu, J. *Polymer* 2003, 44, 2773.
- Fayolle, B.; Audouin, L.; Verdu, J. *Polymer* 2004, 45, 4323.
- Mathur, A. B.; Mathur, G. N. *Polymer* 1982, 23, 54.
- Yue, C. Y.; Msuya, W. F. *J Mater Sci Lett* 1990, 9, 985.
- Viebke, J.; Elble, E.; Ifwarson, M.; Gedde U. W. *Polym Eng Sci* 1994, 34, 1354.
- Dudic, D.; Kostoski, D.; Djokovic, V.; Stojanovic, Z. *Polym Degrad Stab* 2000, 67, 233.
- Mucha, M. *Colloid Polym Sci* 1984, 262, 841.
- Fayolle, B.; Audouin, L.; Colin, X.; Verdu, J. *Polym Degrad Stab* 2007, 92, 231.
- Kakudo, M.; Kasai, N. *X-ray Diffraction by Polymers*; Elsevier Publishing Company: Amsterdam, The Netherlands; New York, USA, 1972.
- Mead, D. W. *J Rheol* 1994, 38, 1797.
- Luftl, S.; Archodoulaki, V.-M.; Seidler, S. *Polym Degrad Stab* 2006, 91, 464.
- Fayolle, B.; Audouin, L.; Verdu, J. *Polym Degrad Stab* 2000, 70, 333.
- Rault, J.; Robelin-Souffaché, E. *J Polym Sci Part B* 1989, 27, 1349.
- Plummer, C. J. G.; Cudré-Mauroux, N.; Kausch, H. H. *Polym Eng Sci* 1994, 34, 318.
- Wu, S. *J Polym Sci Phys Ed* 1989, 27, 723.
- Kennedy, M. A.; Peacock, A. J.; Mandelkern, L. *Macromolecules* 1994, 27, 5297.